# MATERIAL DEFECTS IN A PM-NICKEL-BASE SUPERALLOY

B. Nowak, H. Lahodny*, E. Arzt*,
G. König and E. Affeldt

*Max Planck-Institut für Metallforschung
Stuttgart, FRG
MTU Motoren- und Turbinen-Union München GmbH
Munich, FRG

## Abstract

The purpose of this work was the determination of the type, size and frequency of defects in a nickel-base superalloy (U700). In order to obtain a higher frequency of defects compared to the standard material the alloy was deliberately doped with organic defects (rubber particles). Eight different types of defects were documented and their influence on the surrounding material investigated by energy and wavelength dispersive X-ray analysis.

With the aid of a fully automated scanning device the intersection areas of the defects were determined (shape and size of the circumferential ellipses and the distribution of linear intercepts). The spatial defect size distributions were derived from the distributions of intercept areas and evaluated statistically. The resulting defect distributions were compared to those of unsieved powder.

## 1 Introduction

In modern aero-engines high strength nickel-base alloys are used for disc applications. In the production of these alloys the limitation of the number and size of defects is of fundamental importance. Defects such as pores as well as reactive and nonreactive inclusions are preferred sites for crack initiation. They are the reason for a considerable scatter in measured fatigue lives. Process control measures, especially the sieving of powders before hipping, are able to reduce the maximum size of material defects. The assessment of the influence of defects on the fatigue life requires knowledge of the type, size and frequency of defects.

## 2 Experimental procedure and statistical evaluation

U700 (HIP) has a nominal composition (in weight %) of 0.04 C, 16 Cr, 18 Co, 5.5 Mo, 3.7 Ti, 4.2 Al, 0.03 B, 0.06 Zr and balance Ni. The material was doped with organic defects (particles of fluorocarbon rubber; tradename VITON) with a concentration of 10 mg per kg powder and a size $\leq$ 150 micron. The chemical analysis of the rubber revealed the following metallic constituents (weight %): 2.0 Zn, 0.5 Ca, 0.05 Mg and 0.02 Fe.

Metallographic sections were taken and statistically evaluated with respect to material defects. The spatial size distribution was derived using the following approach: The intersect areas of the defects were described by ellipses and subsequently approximated by circles with diameters equal to the long axis of the ellipses. From the distribution of the intersect-circle diameters the distribution of spheres was calculated (tomato salad problem) according to a method described by Exner (1972); see Fig. 1.

## 3 Results

The following types of defects were established:

a) Pores

Pores were found at triple points of grains and within grains. Pores have the highest frequency and smallest size of all defects (500 defects per cm$^2$; defect size $\leq$ 34 micron; see Fig. 7).

b) Ellipsoid reactive inclusion

A number of defects were found which are characterized by an ellipsoid reaction zone larger than the particle size:

- $\gamma'$ -agglomerations have the largest size of all the reactive inclusions (Figs. 2a and 3); Rings of Ti (C, N) and Mo-rich $M_6C$ (Fig. 2b); Cr-inclusions (Fig. 2c); $ZrO_2$-inclusions (Fig. 2d); Nb/Ti-inclusions (Fig. 2e) and $Al_2O_3$-inclusions (Fig. 2f)

These defects have a lower frequency but a greater size than the pores (3.5 defects per cm$^2$; defect size $\leq$ 229 micron).

c) Viton defects

Organic nonmetallic inclusions are characterized by pronounced prior particle boundaries (Fig. 5). In the defect area and reaction zone the chemical compositions (Fig. 6) and hardness (Fig. 4) differ from the matrix. Viton defects have the lowest frequency and the greatest size of all defects (0.25 defects per cm$^2$; defect size $\leq$ 388 micron).

## 4 Summary and conclusions

In a model alloy (U700 doped with Viton) eight type of defects have been analyzed. The defects can be categorized in three classes: .

- pores
- ellipsoid reactive inclusions
- Viton defects

Pores and reactive inclusions were described by ellipsoids. Viton defects, the largest defects, show a rather irregular shape. Furthermore, they can be distinguished from the matrix by a much higher value of hardness. For that reason a marked influence of fatigue life may be expected. König (1984) has studied the effect of all these defects on the fatigue behaviour. The Viton defects reduced the fatigue life by more than a factor of 10 compared with undoped material.

Fig. 7 gives a summary of the frequency of defects as a function of size. For comparison, typical frequencies of defects in U700 of both sieved and unsieved powders are included. The diagram suggests that the number of reactive zones is about one decade higher than for defects in unsieved powder. However, if the fact is taken into account that the inclusions themselves are about one half of the reactive zone size, there is a reasonable correlation of the defect frequencies.

## 5 References

Betz, W. (1986), In: High Temperature Alloys for Gas Turbines and other Applications 1986. Proceedings of a Conference, Liege, Belgien, 6 - 9 Okt., 81

Exner, H.E. (1972), Int. Metall. Rev. 17, 25 - 42

König, G.W. (1984), In: PM Aerospace Materials, A Metal Powder Report Conference, MPIF, Bern, 12 - 14 Nov., 23

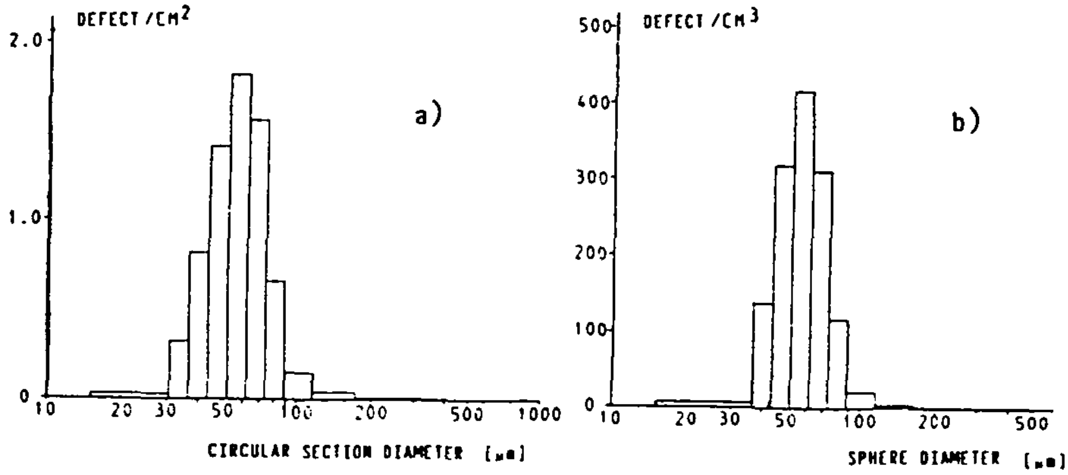

Fig. 1:

Representative defect size distribution
a)two-dimensional
b)three-dimensional

Fig. 2: ELLIPSOID REACTIVE INCLUSIONS

Coarse (1-4um) $\gamma'$-precipitates are not observed on grain boundaries and in grains within the reaction zone.

Measurement section area: $100\ cm^2$

Measured defect count: 346

Lower measurement limit: 21 µm

Max. defect size: 229 µm

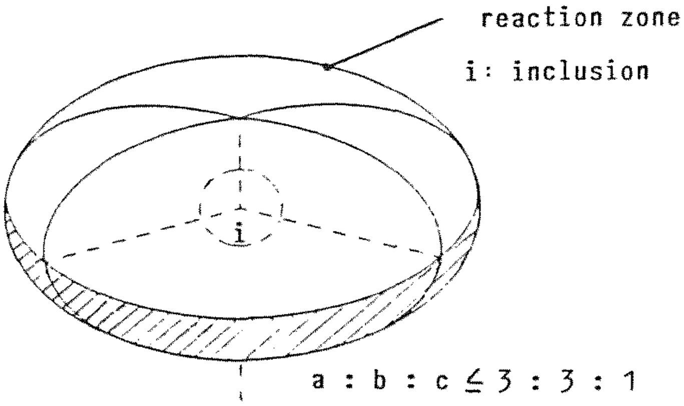

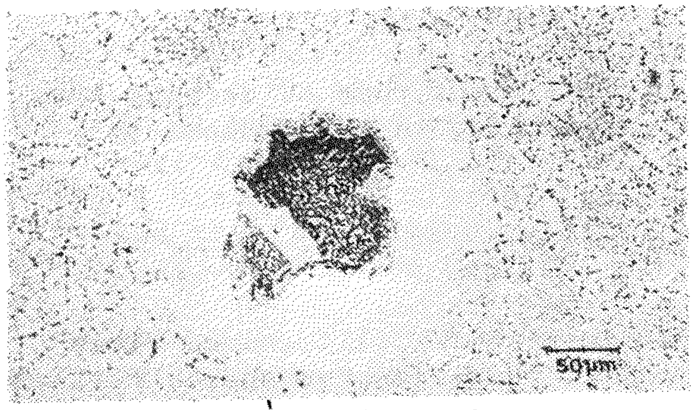

Fig. 2a: $\gamma'$ - agglomeration

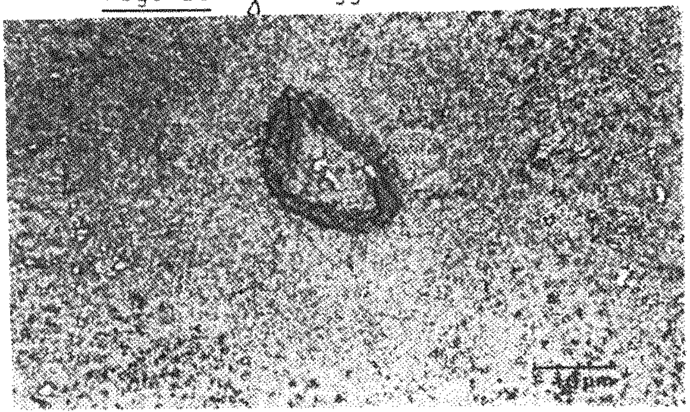

Fig. 2b: Ti(C,N) - ring with molybdenum rich $M_6C$

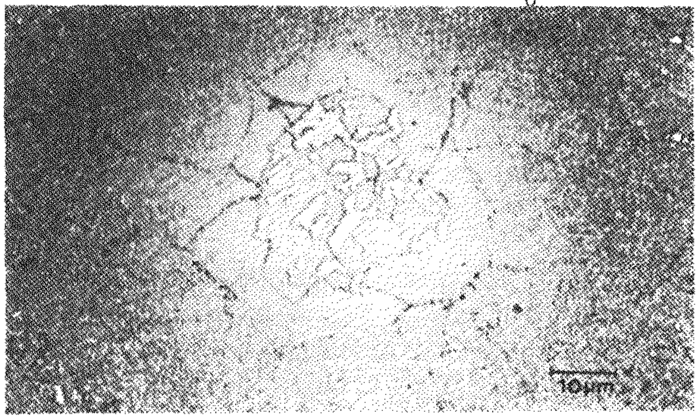

Fig. 2c: Cr - inclusion

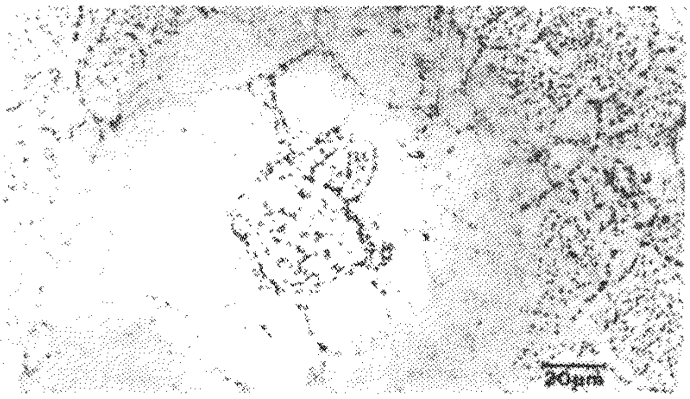

Fig. 2e: Nb/Ti - rich carbide

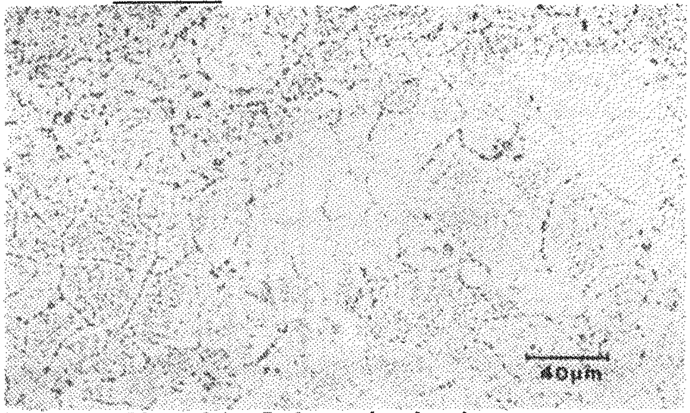

Fig. 2d: $ZrO_2$ - inclusion

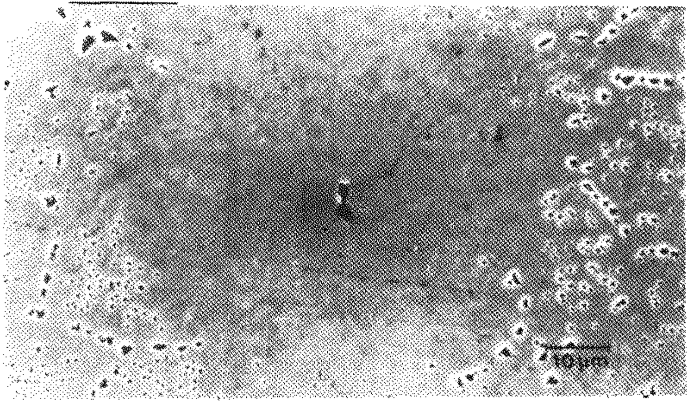

Fig. 2f: $Al_2O_3$ - inclusion

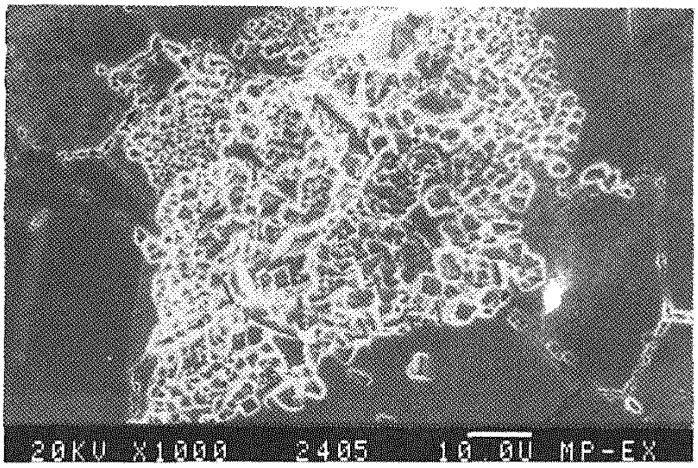

Fig. 3: $\gamma'$ - AGGLOMERATIONS

Energy dispersive x-ray analysis (EDX) shows a higher concentration of $\gamma'$ - formers (Ni, Al and Ti) in the defects than in the matrix. These types of defects can be observed after etching ( Kallings - Adler 1:1; negative etch for $\gamma'$ - precipitates). After a strong etch, cube shaped holes appear where the $\gamma'$ - precipitate was dissolved.

Fig. 4: HARDNESS GRADIENT OVER THE CROSS SECTION

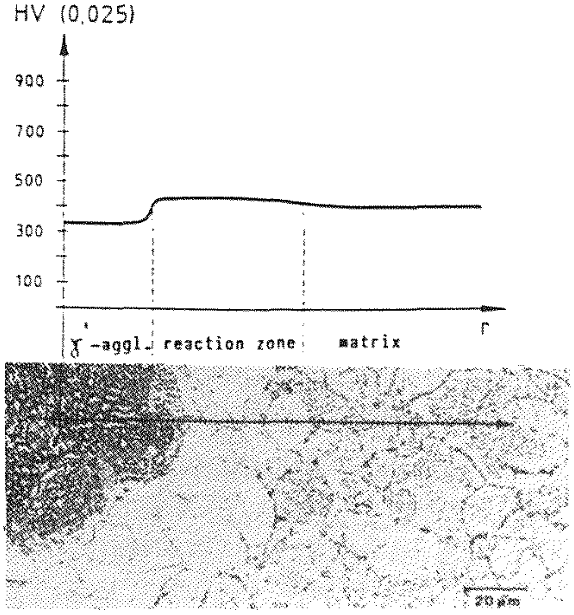

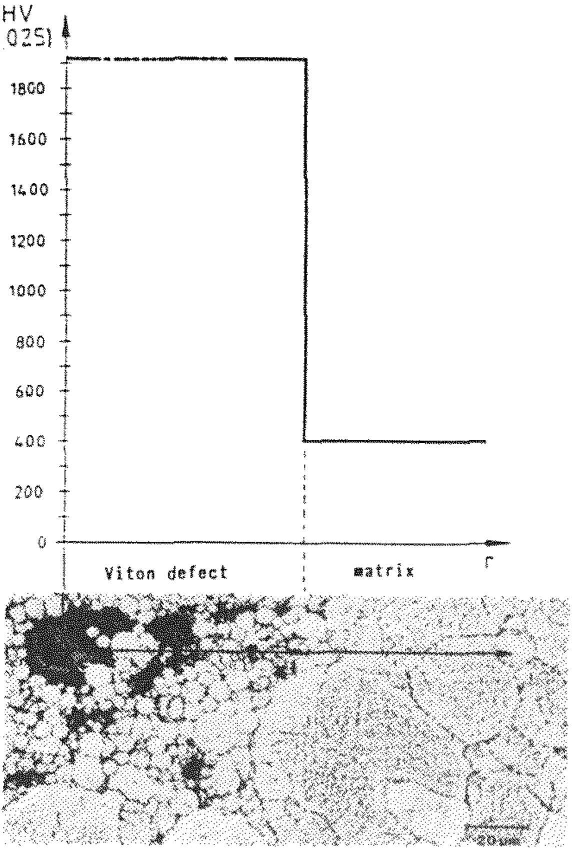

Fig. 5: VITON DEFECTS

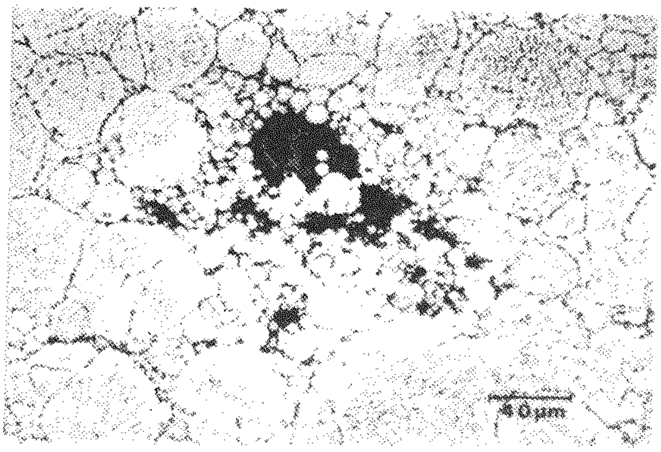

Decoration of prior particle boundaries with carbides and/or oxides.

Measurement section area: 100 $cm^2$

Measured defect count: 25

Lower measurement limit: 39 µm

Max. defect size: 388 µm

Fig. 6: VITON DEFECT

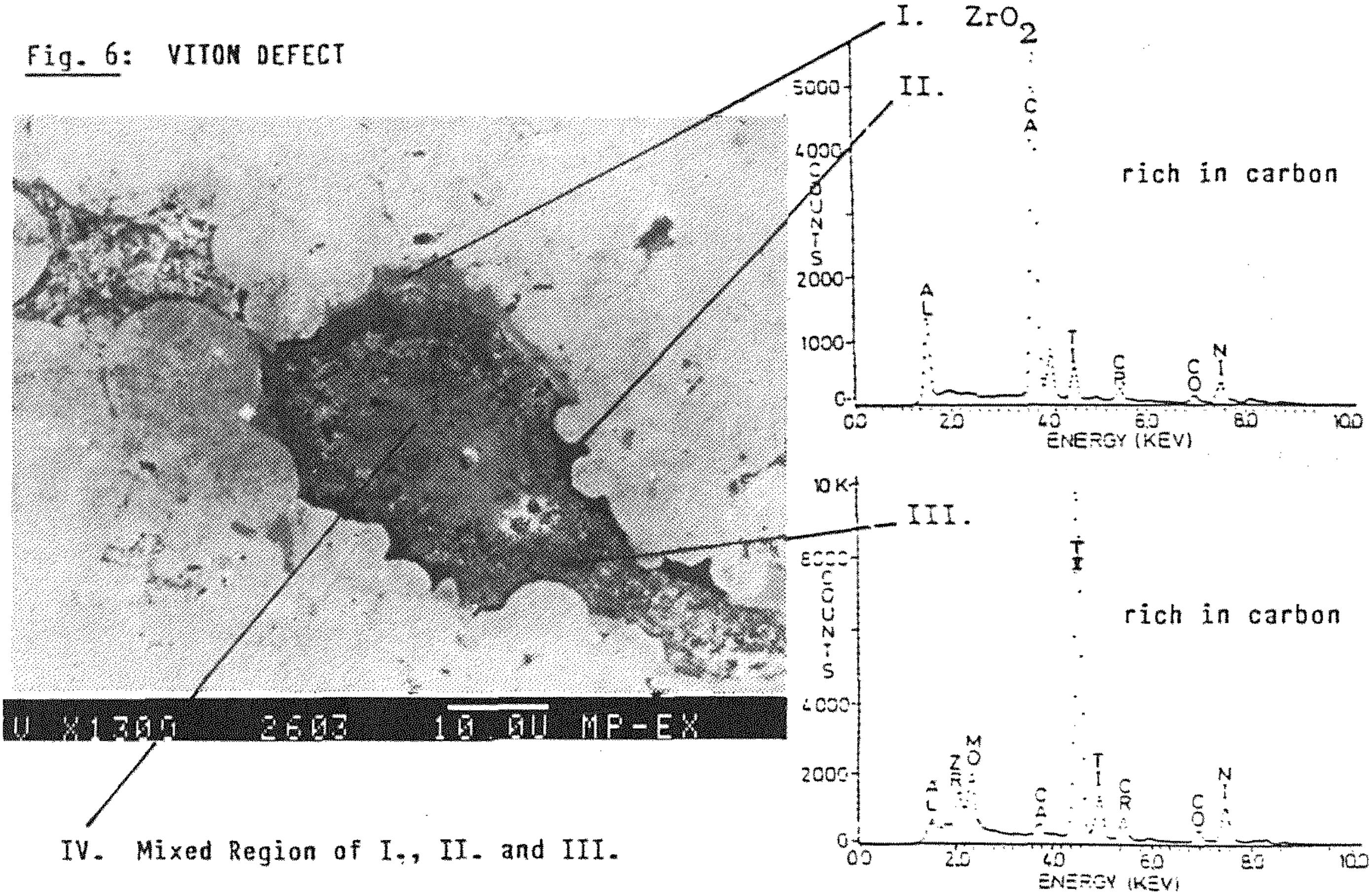

Viton is a source of oxygen and carbon. During HIPing, freed oxygen and carbon react with matrix alloying elements Al, Zr, Ti and Mo to form a compact inclusion. The inclusion contains oxides and carbides, and is surrounded by a reaction zone. Within the reaction zone, the prior powder particle boundaries are covered with aluminium oxide and titanium carbide particles.

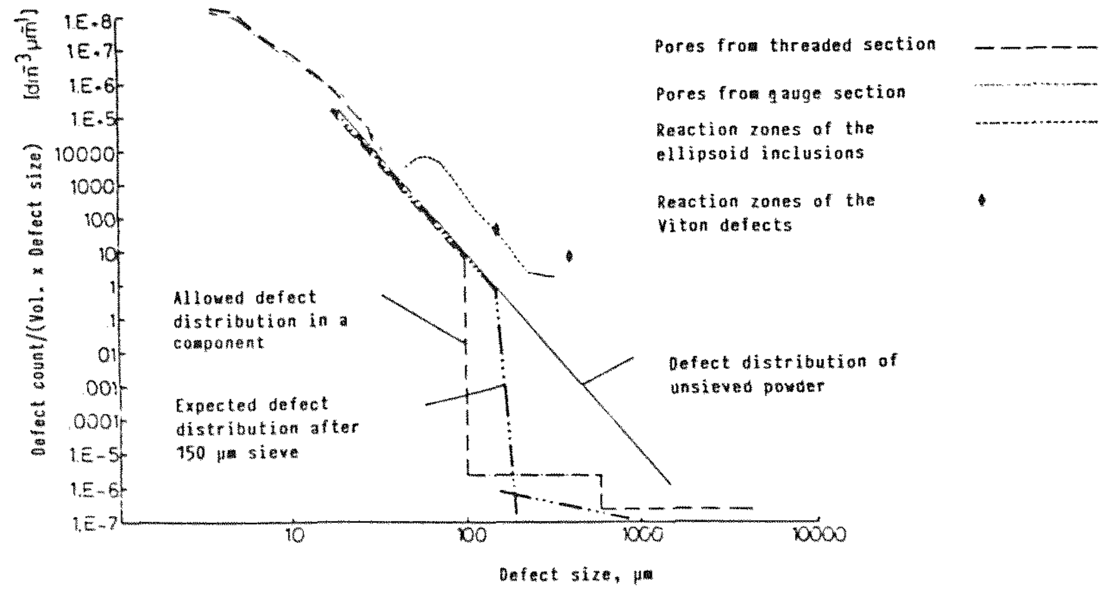

Fig. 7: Comparision of the distribution of sphere diameters with type defect distributions of UDIMET 700 according to Betz (1986).